Redox Biology 53 (2022) 102328

Contents lists available at ScienceDirect

Redox Biology

journal homepage: www.elsevier.com/locate/redox

AKAP12 ameliorates liver injury via targeting PI3K/AKT/PCSK6 pathway

Xuan Wu [a,b,c,1], Yuhong Luo [d,1], Shan Wang [c,e,1], Yueying Li [b], Meiyu Bao [b], Yuanjiang Shang [b], Lei Chen [c,**], Weiwei Liu [a,b,*]

[a] Department of Laboratory Medicine, Longhua Hospital, Shanghai University of Traditional Chinese Medicine, Shanghai, 200032, China
[b] Central Laboratory and Department of Laboratory Medicine, Shanghai Tenth People's Hospital, School of Medicine, Tongji University, Shanghai, 200070, China
[c] International Co-operation Laboratory on Signal Transduction, Eastern Hepatobiliary Surgery Institute, Second Military Medical University, Shanghai, 200438, China
[d] Laboratory of Metabolism, Center for Cancer Research, National Cancer Institute, National Institutes of Health, Bethesda, MD, 20892, USA
[e] Fudan University Shanghai Cancer Center, Shanghai Medical College, Fudan University, Shanghai, 200032, China

ARTICLE INFO

Keywords:
AKAP12
PCSK6
Inflammatory factor
Macrophage infiltration
Liver injury

ABSTRACT

A kinase anchor protein 12 (AKAP12) is a scaffold protein that is critical for cell structure maintenance and signal transduction. However, the role of AKAP12 in liver injury remains unclear. Here, we attempt to explore the potential contribution of AKAP12 in liver injury and elucidate its underlying molecular mechanism. We found that *AKAP12* deletion in acute liver injury (ALI) activates the PI3K/AKT phosphorylation signaling pathway, induces the increased expression of PCSK6 and its downstream inflammation-related genes, and prompts macrophages to produce a large number of inflammatory factors. And knockdown of PCSK6 by in *vivo* siRNA assay reversed in liver injury $AKAP12^{\Delta hep}$ mice, demonstrating that PCSK6 has an important role in ALI. Furthermore, we found that signal transducer and activator of transcription 3 (STAT3) and serine/threonine kinase Akt (AKT) were upregulated in $AKAP12^{\Delta hep}$ mice of chronic liver injury. To sum up, our study here demonstrates that AKAP12 has a protective role in ALI and chronic liver fibrosis, at least in part through inhibition of the PI3K/AKT/PCSK6 pathway. Our findings provide a new potential treatment for liver injury with important clinical implications.

1. Introduction

A-kinase anchor protein 12 (AKAP12)/Src-suppressed C-kinase substrate (SSeCKS) is a member of the AKAP family and a component of the cytoskeleton structure [1]. AKAP12 maintains the stability of cells and tissues, and regulates cell proliferation and metastasis through activation of the phosphoinositide 3-kinase (PI3K)/protein kinase B (AKT) or protein kinase A (PKA)/protein kinase C (PKC) pathways [1–4].

AKAP12 is reportedly decreased, to varying degrees, and closely related to a poor prognosis and high recurrence rate in cancers of the prostate, breast, liver, and lung [5–8]. AKAP12 acts as a regulator of mitosis by anchoring key signaling proteins, such as PKA, PKC, and cyclins, thereby inhibiting the viability of tumor cells and inducing apoptosis via caspase-3 [4,9,10]. Notably, AKAP12 is reportedly downregulated in hepatocellular carcinoma (HCC) via promoter hypermethylation [11–14] and reduced in hepatic cirrhosis and precancerous lesions via upregulation of microRNA (miR)-183 and miR-186, which both target AKAP12. In addition, miR-1251-5p negatively regulates AKAP12 expression and plays a carcinogenic role in HCC [12]. Collectively, these findings indicate that AKAP12 acts a tumor suppressor in liver tumorigenesis.

Since AKAP12 protects against liver fibrosis and HCC progression [7,15,16], it is reasonable to speculate that AKAP12 could influence acute liver failure and hepatocyte death [12,17]. Hence, the potential function and mechanism of AKAP12 in hepatocytes during acute liver injury (ALI) and chronic liver fibrosis were explored using hepatocyte-specific *AKAP12* knockout ($AKAP12^{\Delta hep}$) mice. The results showed that disruption of *AKAP12* in hepatocytes dramatically aggravated acute and chronic liver injury in a proprotein convertase subtilisin/kexin type 6 (PCSK6)-dependent manner.

PCSK6, also named PACE4, is a member of the encoding subtilisin-like proprotein convertase family [17,18]. The protease encoded by PCSK6 is expressed in many tissues, including the liver, intestine, and brain [18]. The PCSK6 gene is believed to affect the production of

* Corresponding author. Department of Laboratory Medicine, Longhua Hospital, Shanghai University of Traditional Chinese Medicine, Shanghai, 200032, China.
** Corresponding author.
E-mail addresses: chenlei@smmu.edu.cn (L. Chen), weiweiliu@shutcm.edu.cn (W. Liu).
[1] These authors contributed equally to this work.

https://doi.org/10.1016/j.redox.2022.102328
Received 5 March 2022; Received in revised form 5 April 2022; Accepted 2 May 2022
Available online 6 May 2022

Abbreviations

ALI	Acute liver injury
AKAP12	A kinase anchor protein 12
PCSK6/PACE4	Proprotein convertase subtilisin/kexin type 6
LPS	Lipopolysaccharide
GalN	Galactosamine
CCL4	Carbon tetrachloride
ROS	Reactive oxygen species
siRNA	small interference RNA
HCC	Hepatocellular carcinoma
AKAPS	A kinase anchoring protein
PI3K	phosphatidylinositol 3 kinase
AKT	serine/threonine kinase Akt/protein kinase B
ALT	Alanine aminotransferase
AST	Aspartate aminotransferase
WB	Western Blot
IL-6	Interleukin-6
IL-1β	Interleukin 1β
TNF-α	Tumor necrosis factor-α
TIMP	Tissue inhibitor of metalloproteinase
α-SMA	α-smooth muscle actin
Col-1α1	Collagen type 1 alpha 1 chain
NAC	N-acetyl cysteine
Bcl-2	B-cell lymphoma-2
Bax	Bcl-2 associated X protein
RASF	Rheumatoid arthritis synovial fibroblast
LSECs	Liver sinusoidal endothelial cells
STAT3	Signal transducers and activators of transcription 3
ERK	Extracellular regulated protein kinases
JNK	C-Jun N-terminal kinase.

inflammatory factors and to play a role in tumor progression [19]. However, no study has yet analyzed the role of PCSK6 in ALI, and the relationship between AKAP12 and PCSK6 remains unclear.

ALI is the initial cause of most liver diseases. Elevated levels of alanine aminotransferase (ALT) and aspartate aminotransferase (AST) are established diagnostic markers of ALI [20,21]. ALI can cause inflammatory storms and even lead to death [22,23]. Although the importance of preventing ALI and liver failure has been recognized for several decades, treatment to relieve symptoms is the most effective approach, as targeted therapies are lacking. At present, there is an urgent need for the identification of potential targets and development of ALI-targeted drugs. Hence, the aim of this study was to explore the potential function and mechanism of AKAP12 in hepatocytes during ALI and chronic liver fibrosis using *AKAP12*$^{\Delta hep}$ mice to develop novel drug target for treatment.

2. Material and methods

2.1. Animals

The original AKAP12 knockout mouse was obtained from JiCuiYaoKang company in Nanjing, China. (C57BL/6 N genetic background). An alb-Cre tool mouse was provided by the Model Animal Research Center of Nanjing University in Nanjing, China. The breeding environment was standardized. (25 °C, 55% humidity, 12 h daylight and 12 h day/night light cycles). F1 generation mice, (AKAP12 systemic knockout mice) were crossed with alb-Cre tool mice to obtain F2 generation mic F2 generation mice were then crossed with one another Finally, F3 generation mice (*AKAP12* $^{fl/fl}$ *and AKAP12*$^{\Delta hep}$) were obtained as the target mice. All experimental steps were supported by the Institutional Animal Care and Use Committee of Tenth's People Hospital (Shanghai, China) and the Use Committee of Second Military Medical University (Shanghai, China).

2.2. Animal model of liver injury

For the liver acute or chronic injury model, 8- to 10-week-old *AKAP12* $^{fl/fl}$ and *AKAP12*$^{\Delta hep}$ male mice were used. Galactosamine (GalN Sigma, USA) was administered intraperitoneally at a dose of 800 mg/kg. Lipopolysaccharide (LPS) was then administered intraperitoneally at 20 μg/kg or 5 μg/kg (Sigma). The blank control group was given an equal volume of physiological saline via the abdominal cavity. After intraperitoneal administration of GalN/LPS, the survival rate of mice was measured (n = 8–12 per group). For the ALI model, carbon tetrachloride (CCl4) was administered by intraperitoneal injection at a dose of 4 ml/kg. The liver fibrosis model involved treatment with CCl4 mixed with olive oil (1:9 v/v), three times per week for 10 weeks. Lastly, *siPCSK6* was injected intravenously (40 nmol per mouse).

2.3. Cell line construction and RNA interference

The mouse HCC cell line Hepa 1-6 was cultured in a 37 °C, 5% CO2 environment. The production of lentivirus for stable cell line construction was completed by GenePharma (Shanghai, China). For RNA interference, siRNA was purchased from GenePharma (Shanghai, China). Lipofectamine™ 3000 Transfection Reagent (L3000015 Thermo Fisher, Waltham, MA, USA) was used to transfect (si) RNA.

2.4. Immunohistochemical (IHC) analysis

Liver specimens were dewaxed, soaked in H_2O_2 for 20 min, washed three times with water, and incubated with an acid repair antigen for 5 min at 100 °C. Afterward, the specimens were washed three times, treated with blocking solution containing 1% bovine serum albumin for 30 min, and probed with a primary antibody overnight at 4 °C. The next day, the specimens were washed four times with phosphate-buffered saline (PBS) and probed with a secondary antibody for 30 min at 37 °C. After washing with PBS, the specimens were stained with 3,3′-diaminobenzidine (DAB) followed by hematoxylin for 10 min. Following dehydration, the specimens were coated with 50 μL of neutral resin.

2.5. Tissue protein extraction

Tissue samples (20 mg) were collected, frozen in liquid nitrogen, ground into powder, and placed in 1.5-mL centrifuge tubes. Following the addition of 1 mL of lysis buffer (P0013J Beyotime Institute of Biotechnology, Haimen, China), the samples were homogenized for 30 s at 1500×*g*, then centrifuged for 30 min. The supernatant was collected for further analysis.

2.6. Terminal deoxynucleotidyl transferase dUTP nick end labeling (TUNEL) assay to assess apoptosis

After full deparaffinization and hydration, the samples were incubated with proteinase K solution for 10–30 min, washed with PBS, and incubated with TUNEL reaction solution for 1 h at 37 °C. Afterward, the samples were immersed in 0.3% H_2O_2 for 15 min, washed three times with PBS, reacted with 100 μL of horseradish peroxidase-conjugated streptavidin (diluted to 1:500 in PBS) for 30 min, then washed three times for 5 min with PBS. Finally, the samples were stained with DAB for 10 min, washed with PBS, and coated with neutral resin.

2.7. Isolation of mouse primary hepatocytes

Mouse livers were perfused with egtazic acid solution for 1–2 min at a flow rate of 5 mL/min, followed by pronase solution for 5 min and then infused with collagenase solution for 7 min. Afterward, the liver tissue was minced with 5 mL of pronase/collagenase solution and 1% DNase, then placed in a sterile petri dish. Following centrifugation at 180 rpm for 25 min, the tissue was filtered once through a 7-μm cell strainer and then centrifuged at 50×*g* for 10 min at 4 °C. After aspiration of the supernatant, the cells were suspended in 120 μL of DNase I, then washed and centrifuged at 50×*g* for 10 min at 4 °C.

2.8. mRNA level analysis

Mouse liver tissue was collected, added to Trizol, and stored at -80 °C until total RNA was extracted. The tissue was homogenized with ceramic beads, then RNA was extracted and reverse-transcribed into cDNA. The obtained cDNA was used for quantitative PCR (CFX96/384 TouchTM, Bio-Rad). Prior to use, each set of primers (Table 1) and RT-PCR conditions were extensively optimized to improve the efficiency of the reaction and avoid interference from primer dimers. The cycle parameters were as follows: 1 min at 65 °C, 45 cycles of 30 s at 94 °C, 1 min at 59 °C, and 1 min at 72 °C. Real-time quantitative PCR data were normalized to reference geneβ-actin expression using the $2^{-\Delta\Delta Ct}$ method.

2.9. Statistical analysis

Statistical analyses were conducted using GraphPad Prism 7.0 software (GraphPad Software, Inc., San Diego, CA, USA). Values are expressed as the mean ± standard error. The two-tailed Student's *t*-test was used to identify significant differences between two groups. Comparisons were made using the two-tailed paired *t*-test. A probability (*p*) value of <0.05 was considered statistically significant.

Table 1
Primer sequence.

Gene		Sequences (5′-3′)
m-PCSK6	**Forward**	**CAGGCGCGAAGTGACTCTC**
	Reverse	**GACCGACAGCGACTGTTCTT**
m-Fut8	**Forward**	**GGTTCCTGGCGTTGGATTATG**
	Reverse	**TCAATGGGGCCTTCTGGTATT**
m-Kif21a	**Forward**	**AAGATCGAAGGTTGCCATATCTG**
	Reverse	**CAGCTCCGGTTTGTCCATAGG**
m-Golgb1	**Forward**	**ATCAGGAGATTACACTGACTGGA**
	Reverse	**GAGCATCCTCTTGCGTGGATT**
m-Zfand6	**Forward**	**GCTCAAGAAACTAATCACAGCCA**
	Reverse	**GGTGGGCTTATTCTACCATTGC**
m-Sertad2	**Forward**	**AAGGAGGAAAACGGAAGTTTGAT**
	Reverse	**TGAAGATAGTCTGGCGCTGTA**
m-Men1	**Forward**	**ACGGTGCAGATTACAGGGGA**
	Reverse	**TTGGGGTACTTCAGCGTGTTG**
m-Trim3	**Forward**	**CCTGGGATTAAATCATGGACCAC**
	Reverse	**TGACAGGACACTTATCAAAGGC**
m-Dtx3	**Forward**	**ACCCAATGTCATCACTTGGAAC**
	Reverse	**CCTCTTGCACCCTAGTCAGGT**
m-Ap3m2	**Forward**	**CCCAAGAGAGAGCTACCGAG**
	Reverse	**GAACAGACCCCAAAATAGTCCTG**
m-β-actin	**Forward**	**GGCTGTATTCCCCTCCATCG**
	Reverse	**CCAGTTGGTAACAATGCCATGT**
m-Bcl 2	**Forward**	**GTCGCTACCGTCGTGACTTC**
	Reverse	**CAGACATGCACCTACCCAGC**
m-cre	**Forward**	**GATGGATGGATGAGATCATAGGAG**
	Reverse	**GAGGCTCAAGAGGCGAAATG**
m-Prkcd	**Forward**	**CTCTTTCCAGTCGTAAAGCAGC**
	Reverse	**CCTTGGTAGGTTGAGGAGGTT**
m-AKAP12	**Forward**	**TGATGGGTGTGGAACACAGG**
	Reverse	**CTTCTAAAGCAGCACAGGATATG**

3. Results

3.1. Knockdown of AKAP12 in hepatocytes exacerbated galactosamine (D-GalN)/lipopolysaccharide (LPS)-induced ALI

Hepatocyte-specific *AKAP12* knockout ($AKAP12^{\Delta hep}$) mice were established by crossing *alb-Cre* mice with $AKAP12^{fl/fl}$ mice. $AKAP12^{\Delta hep}$ mice was validated by real-time quantitative polymerase chain reaction (qPCR) and IHC staining (Supplemental Figs. 1A–C). Subsequently, $AKAP12^{fl/fl}$ and $AKAP12^{\Delta hep}$ mice were subjected to a mouse model of ALI (low concentration group: 800 mg/kg GalN + 5 μg/kg LPS). As shown in Fig. 1A, mice were sacrificed at indicated time points and tissues and serum were collected. Another set of mice were used to assess survival after intraperitoneal injection of drugs to induce ALI (Fig. 1B). The results showed that liver congestion was more severe in the $AKAP12^{\Delta hep}$ group than the $AKAP12^{fl/fl}$ group at 4 h and 6 h (Fig. 1C). The livers of the two groups at 4 h were stained with hematoxylin and eosin (H&E). As shown in Fig. 1D, *AKAP12* deletion was associated with more severe liver damage. Glutathione (GSH) is an important regulator of intracellular metabolism. A decrease in serum GSH content is an established marker of oxygen free radical production and subsequent apoptosis [24,25]. Mouse serum was collected for detection of GSH and the liver function indicators ALT and AST. The results showed that serum GSH was significantly decreased, while serum ALT and AST were significantly increased in $AKAP12^{\Delta hep}$ group (Fig. 1E and F). The causes of liver congestion and necrosis were further investigated. The IHC results revealed that infiltration of F4/80-positive macrophages around the liver sinusoids was relatively increased in $AKAP12^{\Delta hep}$ mice (Fig. 1G). Furthermore, mRNA levels of the inflammatory cytokines interleukin (IL)-1β, IL-2, IL-6, and tumor necrosis factor (TNF)-α were significantly higher in the livers of $AKAP12^{\Delta hep}$ mice as compared with $AKAP12^{fl/fl}$ mice (Fig. 1H). Finally, the expression levels of pro-apoptotic cleaved poly ADP-ribose polymerase (PARP) and cleaved caspase-3 were increased in $AKAP12^{\Delta hep}$ mice (Fig. 1I). Collectively, these results confirmed that liver damage was more severe in the $AKAP12^{\Delta hep}$ group and that knockout of *AKAP12* promoted liver damage.

Another model of ALI (high concentration group: 800 mg/kg GalN + 20 μg/kg LPS) showed that liver damage was also more severe in the $AKAP12^{\Delta hep}$ group (Supplemental Figs. 2A–E). Together, these results demonstrate that AKAP12 plays an important role in maintaining the stability of cellular structures and resisting damage by ROS.

3.2. Hepatic AKAP12 deficiency aggravates carbon tetrachloride (CCl_4)-induced ALI

To further confirm the role of hepatic *AKAP12* in ALI, a mouse model of CCl_4-induced ALI was constructed (Fig. 2A). Mice were sacrificed at 12 h after intraperitoneal administration of CCl_4 (Fig. 2A). H&E staining of liver tissues demonstrated larger areas of hepatic necrosis in the $AKAP12^{\Delta hep}$ group as compared with the control group (Fig. 2B). TUNEL staining showed that the liver tissues of the $AKAP12^{\Delta hep}$ mice were enriched with apoptotic hepatocytes (Fig. 2C). In addition, serum GSH levels were significantly decreased in the $AKAP12^{\Delta hep}$ group as compared with the control group, indicating early activation of apoptosis (Fig. 2D). Meanwhile, serum levels of ALT and AST were increased in the $AKAP12^{\Delta hep}$ group (Fig. 2E). Finally, qPCR analysis showed that the mRNA expression of the inflammatory factors IL-1β, IL-6, and TNF-α, were significantly increased in the liver tissues of $AKAP12^{\Delta hep}$ mice (Fig. 2F). Taken together, these results suggest that hepatocyte-specific knockout of *AKAP12* triggers more severe liver injury during ALI.

3.3. Loss of AKAP12 results in more severe CCL_4-induced liver fibrosis

The experimental results confirmed that AKAP12 knockout induces

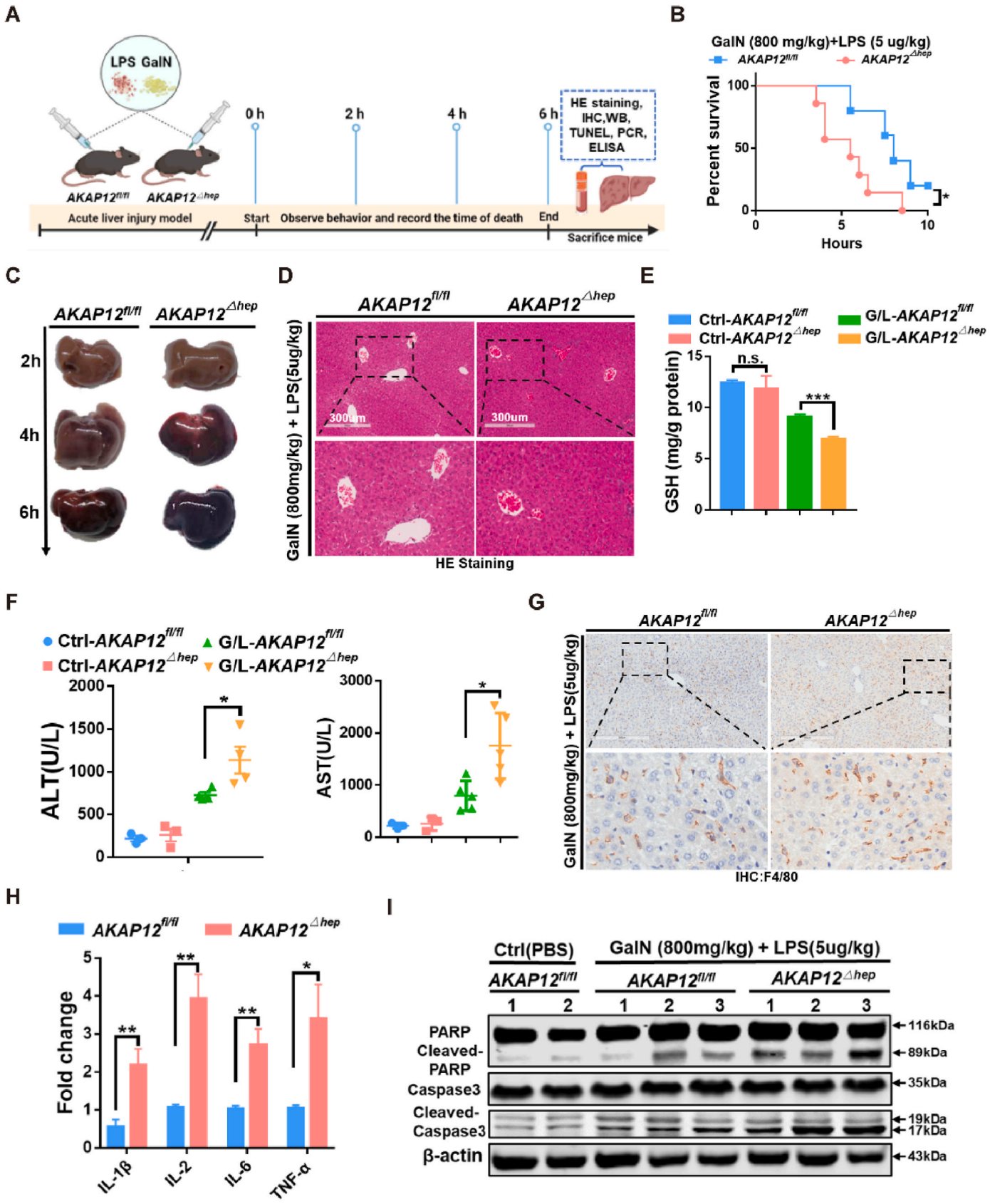

Fig. 1. AKAP12 knockout exacerbates LPS-GalN ALI. (A) Schematic diagram of the mouse experiments. (B) Statistical analysis of survival time (n = 5–8/group). (C) Mouse livers were collected at 2, 4, and 6 h after intraperitoneal injection of 800 mg/kg GalN + 5 μg/kg LPS. (D) H&E staining. (E) Serum levels of GSH(n = 5/group). (F) AST and ALT levels as markers of liver function (n = 5/group). (G) IHC staining. (H) mRNA expression levels of inflammatory factors in liver tissue (n = 3/group).(I) Western blot (WB) analysis of the apoptotic proteins PARP, cleaved PARP, caspase-3, and cleaved caspase-3 (n = 3/group) (*$p < 0.05$, **$p < 0.01$, ****$p < 0.0001$).

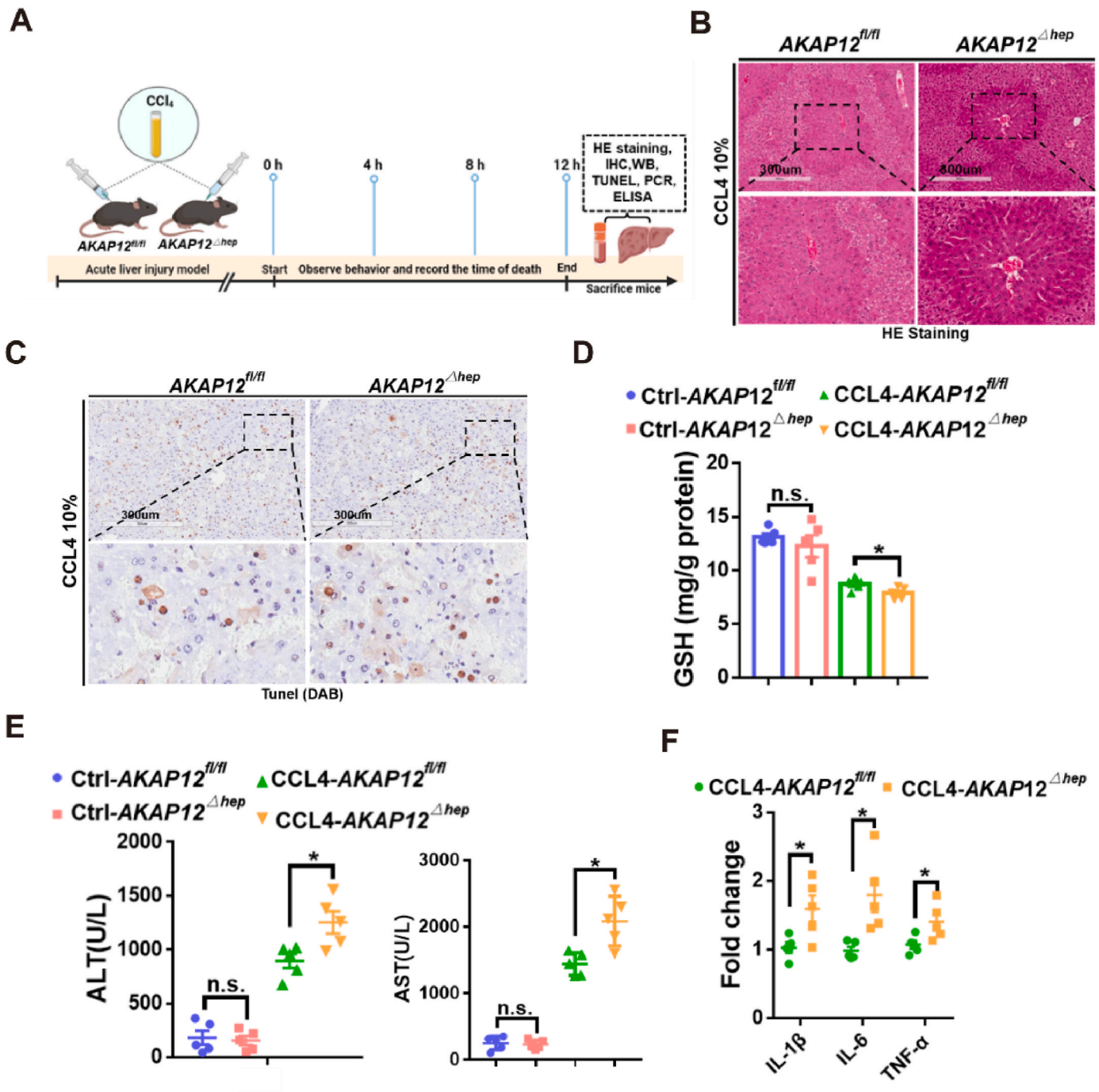

Fig. 2. AKAP12 knockout aggravates CCl_4-mediated ALI. (A) CCl_4-induced acute liver injury model (n = 5–8/group). (B) H&E staining (C) TUNEL staining of apoptotic cells. (D) Serum GSH content (n = 5/group). (E) Serum levels of ALT and AST as indicators of liver function (n = 5/group). (F) Serum levels of inflammatory factors (n = 3/group) (*$p < 0.05$, *n.s.* $p > 0.05$).

more severe liver injury. To further explore the role of AKAP12 in liver fibrosis, *AKAP12*$^{\Delta hep}$ and *AKAP12*$^{fl/fl}$ mice were treated with CCl_4 for 10 weeks. The staining results (Masson, Sirius red, and IHC) demonstrated a dramatically increased level of liver fibrosis in the *AKAP12*$^{\Delta hep}$ group as compared with the *AKAP12* $^{fl/fl}$ group (Fig. 3A–C). Subsequently, markers of early fibrosis and inflammation were detected. The expression levels of α-smooth muscle actin (α-SMA) and tissue inhibitor of metalloproteinase 1 were significantly higher in the liver tissues of the *AKAP12*$^{\Delta hep}$ group than the control group at weeks 2, 4, 6, 8, and 10 (Fig. 3D). The expression levels of inflammatory factors were significantly increased in the liver tissues of *AKAP12*$^{\Delta hep}$ mice (Fig. 3E). WB analysis of α-SMA protein levels confirmed that liver fibrosis was more severe in the *AKAP12*$^{\Delta hep}$ group than the *AKAP12*$^{\Delta hep}$ group at 2, 6, and 10 weeks (Fig. 3F). To further investigate the mechanism by which *AKAP12* deficiency exacerbates liver fibrosis, four pathways closely associated with liver fibrosis were examined. The results showed that signal transducer and activator of transcription 3 (STAT3) and serine/threonine kinase Akt (AKT) were phosphorylated (activated) in the liver tissues of the *AKAP12*$^{\Delta hep}$ group (Fig. 3G). However, there was no significant difference in the expression levels of phosphorylated extracellular regulated protein kinase (ERK) and c-Jun N-terminal kinase (JNK) between the two groups (Fig. 3G). Loss of *AKAP12* activates the p-STAT3 and p-AKT pathways and aggravates liver fibrosis.

(A–C) Liver samples were collected from mice treated with CCl_4 at 0,

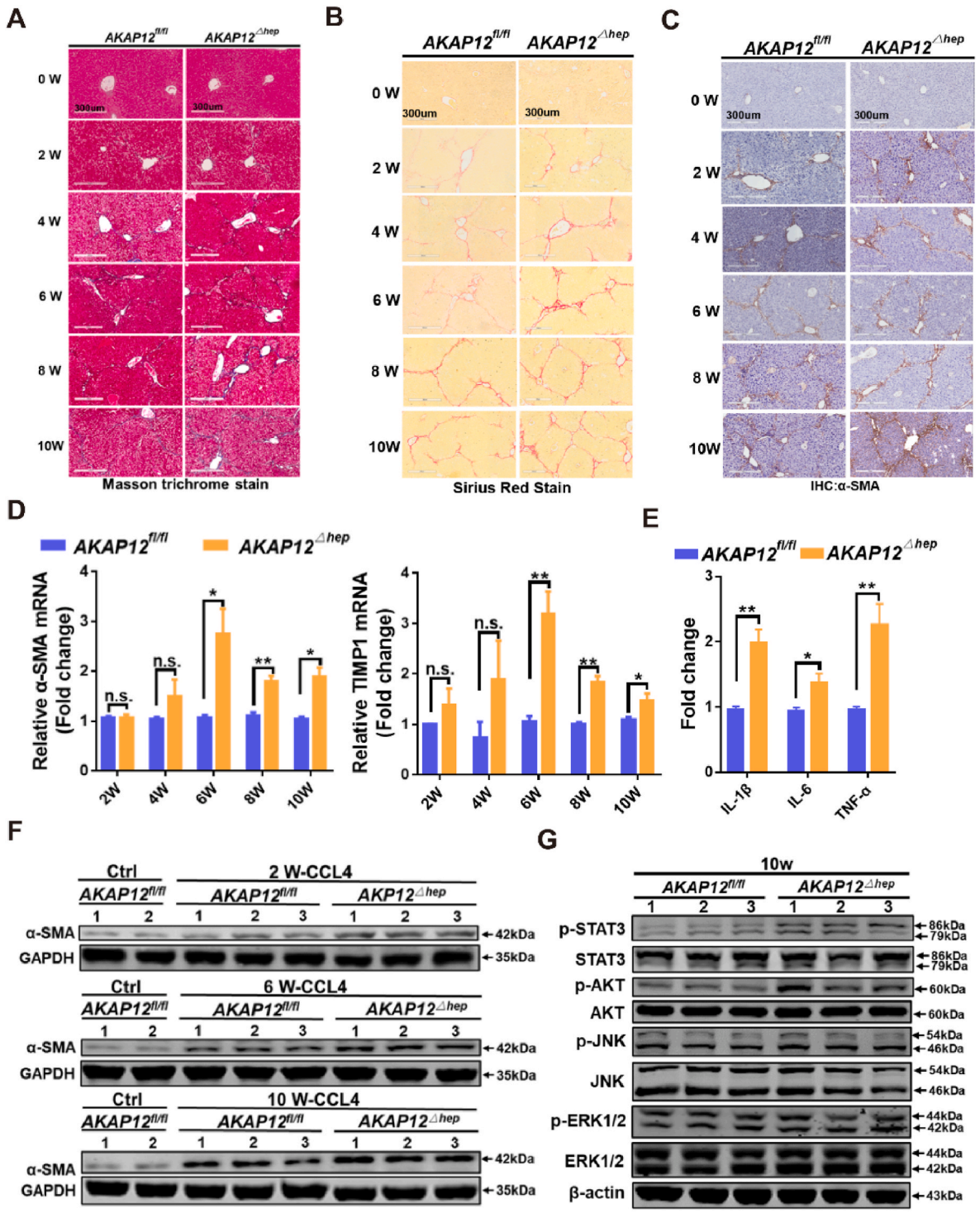

Fig. 3. Knockout of AKAP12 results in more severe CCL_4-induced liver fibrosis.

2, 4, 6, 8, and 10 weeks and stained (Masson trichrome, Sirius red, and IHC). (D) Detection of fibrosis-related genes (n = 3/group). (E) Detection of inflammatory factors (n = 3/group). (F) WB analysis of α-SMA protein expression at 2, 6, and 10 weeks (n = 3/group). (G) Phosphorylation pathway detection (n = 3/group) (*$p < 0.05$, **$p < 0.01$, ***$p < 0.001$, *n.s.* $p > 0.05$).

3.4. Limited role of antioxidants in GalN/LPS-induced ALI of AKAP12$^{\Delta hep}$ mice

The use of antioxidants has potential to alleviate acute liver damage. Therefore, we tested if antioxidant N-acetylcysteine (NAC) could reverse exacerbated ALI in *AKAP12$^{\Delta hep}$* mice. NAC were added to the drinking water of mice 24 h before the experiment, followed by intraperitoneal injection of NAC (150 mg/kg) at 30 min post GalN/LPS dosing. After NAC treatment, H&E staining, liver function and GSH results demonstrated that liver damage was alleviated in both *AKAP12 $^{fl/fl}$* and

AKAP12$^{\Delta hep}$ mice (Fig. 4A–C). However, the expression levels of liver inflammatory factors remained significantly elevated in the *AKAP12*$^{\Delta hep}$ group as compared with the *AKAP12* $^{fl/fl}$ group (Fig. 4D). The IHC staining results demonstrated that the liver tissues of *AKAP12*$^{\Delta hep}$ mice had greater infiltration of macrophages (Fig. 4E). Moreover, the expression levels of apoptotic proteins were significantly elevated in *AKAP12*$^{\Delta hep}$ mice (Fig. 4F).

NAC treatment had no significant effect on high concentration-GalN/LPS and CCL_4 induced ALI. Although liver congestion and necrosis could be relieved, the levels of inflammatory factors in serum were still significantly increased (Supplemental Figs. 3A–D and Supplemental Figs. 4A–E). The results suggested that in addition to oxidative stress, there are other factors that exacerbate liver injury. Taken together, these results revealed that NAC has limited protection against *AKAP12* knockdown-induced ALI and did not effectively reduce the production and infiltration of inflammatory factors, indicating that factors other than ROS trigger liver injury in AKAP12$^{\Delta hep}$ mice.

3.5. PCSK6 is a potential target of AKAP12

RNA sequencing was performed to identify targets of AKAP12. Whole transcriptome sequencing of liver tissues from untreated *AKAP12*$^{\Delta hep}$ and *AKAP12* $^{fl/fl}$ mice (n = 3/group) identified 1275 genes that were upregulated and 987 that were downregulated. The results are presented in a heat map (Fig. 5A) and volcano plot (Fig. 5B). qPCR was performed to verify the changes of the top 10 upregulated genes (Table 2 and Fig. 5C). PCSK6 was the most significantly elevated gene in the liver of *AKAP12*$^{\Delta hep}$ mice and is strongly associated with inflammation and

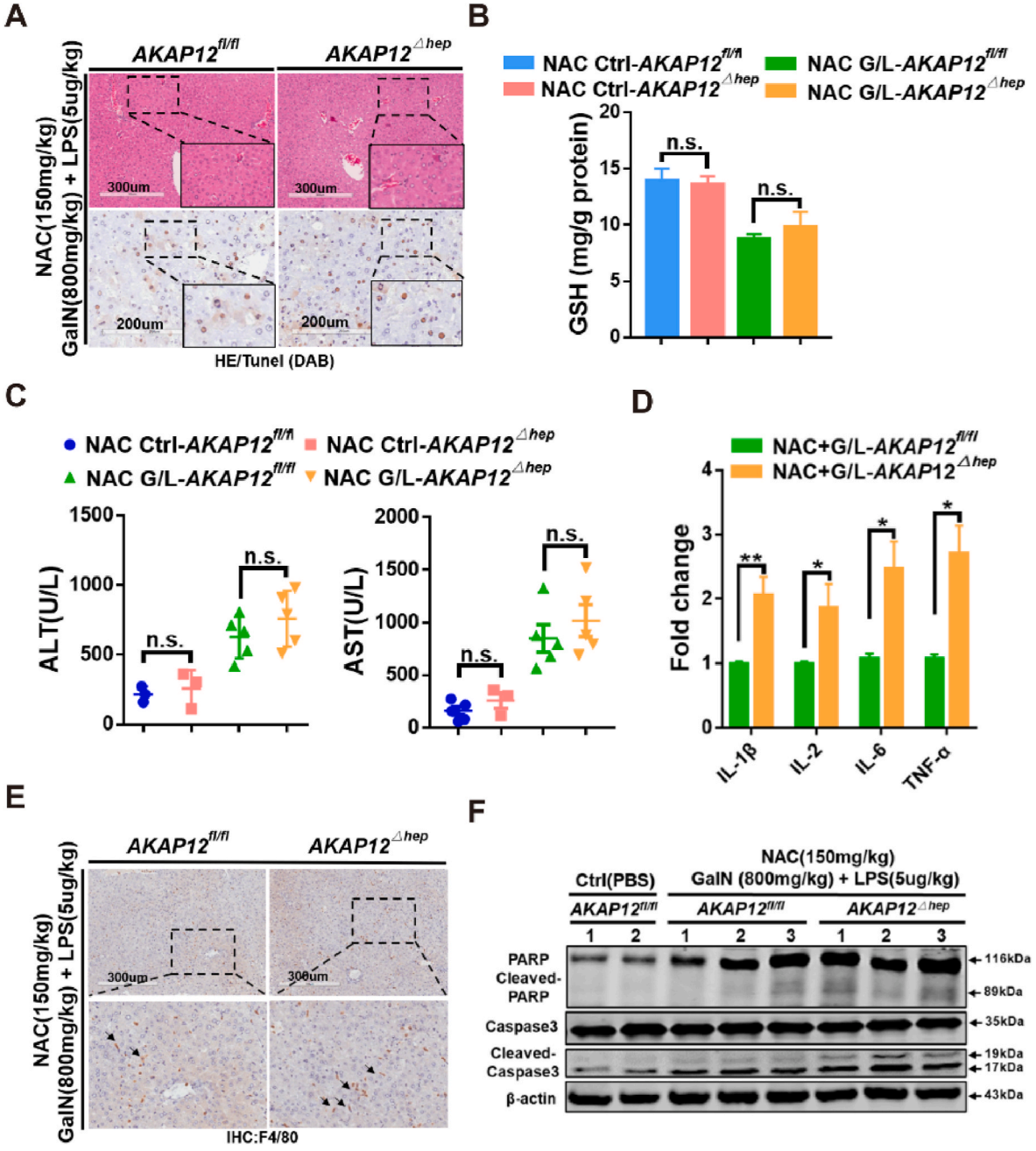

Fig. 4. NAC failed to relieve ALI. (A) Liver tissues were collected from mice with ALI within 4 h of NAC administration (150 mg/kg) for H&E and TUNEL staining (n = 5–12/group). (B) Serum GSH content (n = 5/group). (C) Serum ALT and AST levels (n = 5/group). (D) mRNA expression levels of inflammatory factors in liver tissues (n = 3/group). (E) IHC staining of F4/80. (F) Expression levels of apoptotic proteins in liver tissues (n = 3/group) (*$p < 0.05$, **$p < 0.01$, *n.s.* $p > 0.05$).

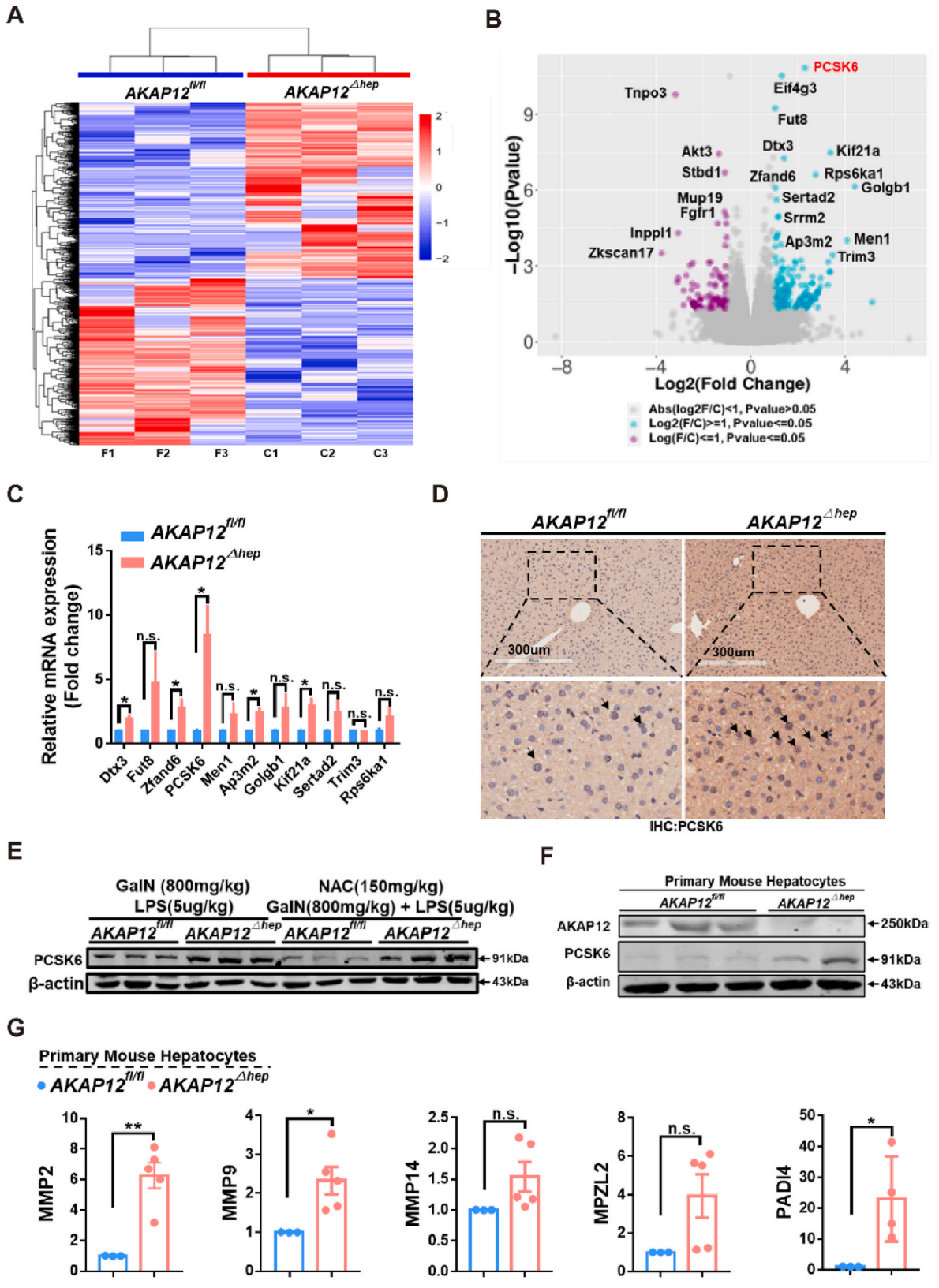

Fig. 5. PCSK6 expression was significantly increased in the liver tissues of *AKAP12*$^{\Delta hep}$ mice. (A) Whole transcriptome sequencing of liver tissues of untreated *AKAP12*$^{\Delta hep}$ and *AKAP12*$^{fl/fl}$ mice (n = 3/group). (B) A volcano map. (C) Verification of mRNA levels (n = 3/group). (D) IHC detection of PCSK6 expression. (E) WB detection of PCSK6 protein expression (F) Protein expression of AKAP12 and PCSK6 in primary hepatocytes of *AKAP12*$^{\Delta hep}$ mice (n = 2–3/group). (G) mRNA expression of PCSK6 downstream genes (n = 3/group) (*$p < 0.05$, **$p < 0.01$, *n.s.* $p > 0.05$).

Table 2
Differential gene list.

Up genes	F1	F2	F3	C1	C2	C3	FoldChange	C_vs_F_Pvalue
Pcsk6	**0**	**0**	**0**	**12.2**	**11.5**	**11.6**	**11.75**	**4.54E-132**
Eif4g3	**0**	**0**	**0**	**10.1**	**10.6**	**8.3**	**9.67**	**2.87E-34**
Fut8	**0**	**0**	**0**	**8.9**	**7.81**	**9.45**	**8.72**	**5.73E-36**
Kif21a	**0**	**0**	**0**	**5.49**	**7.75**	**9.33**	**7.52**	**2.32E-09**
Prkcd	**0**	**0**	**0**	**6.58**	**7.14**	**7.28**	**7**	**4.03E-29**
Rps6ka1	**0**	**0**	**0**	**7.1**	**6.03**	**7.22**	**6.78**	**3.92E-22**
Golgb1	**0**	**0**	**0**	**7.24**	**6.34**	**6.54**	**6.71**	**6.38E-24**
Zfand6	**0**	**3.35**	**5.1**	**9.54**	**9.34**	**9.24**	**6.55**	**6.35E-08**
Sertad2	**2.4**	**0**	**0**	**7.73**	**7.88**	**6.09**	**6.45**	**6.21E-13**
Srrm2	**1**	**1.02**	**1.54**	**11.5**	**11**	**0**	**6.31**	**0.007822695**
Men1	**0**	**3.49**	**0**	**6.66**	**6.89**	**7.34**	**5.8**	**2.38E-05**
Trim3	**1**	**1.02**	**0**	**6.89**	**3.24**	**6.33**	**4.81**	**1.60E-06**
Dtx3	**0**	**0**	**0**	**2.93**	**5.36**	**5.76**	**4.68**	**1.88E-06**
Hook 2	**3.4**	**0**	**1**	**6.04**	**6.16**	**4.96**	**4.6**	**0.001763728**
Ap3m2	**0**	**0**	**0**	**6.66**	**6.28**	**0.83**	**4.59**	**0.002569802**
AU040320	**0**	**0**	**3.64**	**4.59**	**5.36**	**7.38**	**4.57**	**0.012275122**
Tnpo1	**1**	**3.35**	**5.02**	**3.12**	**10.7**	**9.15**	**4.53**	**0.040947987**
Khk	**6**	**5.73**	**6.08**	**10.6**	**10.3**	**10.5**	**4.52**	**9.15E-109**
Ncmap	**0**	**0**	**0**	**5.04**	**4.24**	**4.11**	**4.46**	**8.70E-09**
Exoc3l4	**0**	**0**	**0**	**4.46**	**4.24**	**4.45**	**4.38**	**1.98E-09**
Down genes	**F1**	**F2**	**F3**	**C1**	**C2**	**C3**	**FoldChange**	**C_vs_F_Pvalue**
Tnpo3	**10**	**10.5**	**10.8**	**0**	**2.06**	**2.49**	**-9.06**	**7.94E-121**
Akt 3	**8.9**	**9.09**	**9.24**	**1.68**	**1.63**	**1.35**	**-7.51**	**5.52E-72**
Stbd1	**6.1**	**7.38**	**7.48**	**0**	**0**	**0**	**-6.99**	**1.35E-22**
Mup19	**9.6**	**7.38**	**3.4**	**0**	**0**	**0**	**-6.8**	**0.043743349**
Fgfr1	**6.4**	**7**	**6.67**	**0**	**0**	**0**	**-6.7**	**8.54E-28**
Inppl1	**8.1**	**9.44**	**8.44**	**2.44**	**3.53**	**0**	**-6.69**	**2.43E-14**
Zkscan17	**7.8**	**8.64**	**6.22**	**0**	**0**	**2.84**	**-6.59**	**1.43E-07**
Stat 1	**5.7**	**6.86**	**6.96**	**0**	**0**	**0**	**-6.51**	**7.63E-20**
Ppp2r5e	**6.5**	**6.51**	**6.24**	**0**	**0**	**0**	**-6.42**	**2.75E-26**
C2cd3	**6.5**	**5.91**	**6.12**	**0**	**0**	**0**	**-6.19**	**4.00E-22**
Synpo	**3.4**	**7.13**	**7.58**	**0**	**0**	**0**	**-6.03**	**1.82E-06**
Tubd1	**6.4**	**6.18**	**5.26**	**0**	**0**	**0**	**-5.93**	**4.83E-17**
Srl	**6.6**	**6.64**	**6.27**	**0**	**0**	**1.73**	**-5.92**	**3.87E-24**
Bend 4	**5.8**	**6.42**	**5.49**	**0**	**0**	**0**	**-5.91**	**7.66E-18**
Ilvbl	**5.8**	**5.61**	**6.26**	**0**	**0**	**0**	**-5.9**	**1.82E-19**
Poli	**7.1**	**6.35**	**5.18**	**0**	**1.04**	**0**	**-5.87**	**9.91E-14**
Pus 10	**8.4**	**7.55**	**8.91**	**4.46**	**1.04**	**2.03**	**-5.78**	**8.59E-09**
Tipin	**7.1**	**7.78**	**7.25**	**4.04**	**0**	**0.83**	**-5.74**	**4.57E-05**
Fign l2	**8.4**	**5.94**	**7.75**	**2.44**	**1.63**	**0.83**	**-5.72**	**1.40E-13**
Pds5b	**6.5**	**7.05**	**6.75**	**3.3**	**0**	**0**	**-5.68**	**7.22E-06**

autoimmune disease [26,27] (Fig. 5C). PCSK6, which is expressed in various tissues, including the liver, intestine, and brain [28,29], is reported to affect the production of inflammatory factors and to play a role in tumor progression. Specific knockout of *AKAP12* in hepatocytes triggered increased PCSK6 expression (Fig. 5D and E). Notably, NAC had no effect on PCSK6 expression (Fig. 5E). Moreover, analysis of primary hepatocyte confirmed that knockout of *AKAP12* promoted elevation of PCSK6 protein expression (Fig. 5F). In addition, several studies have reported that increased *PCSK6* induces increased expression of downstream inflammation-related genes [30,31]. In the present study, the downstream target genes of PCSK6, including matrix metallopeptidase 2 (MMP2), MMP4, MMP9, and peptidyl arginine deiminase 4, were significantly increased in the liver tissues of $AKAP12^{\Delta hep}$ mice (Fig. 5G). These results suggested that AKAP12 inhibited expression of PCSK6.

3.6. AKAP12 knockout activated the PI3K/AKT pathway and promoted PCSK6 expression, thereby exacerbating ALI

Various cell lines (*PCSK6* silenced, *AKAP12* silenced, *AKAP12* overexpressed, and *PCKS6/AKAP12* silenced) were constructed to explore the mechanism underlying regulation between AKAP12 and PCSK6. Silencing of PCSK6 reduced PCSK6 expression, but had no effect on the expression levels of AKAP12, PI3K, and AKT (Fig. 6A). To further explore the interaction between PCSK6 and AKAP12, a stable knockdown *AKAP12* cell line was constructed using lentiviral transfection. Knockdown of *AKAP12* was verified by qPCR and WB analyses (Fig. 6B and C). Consistent with the *in vivo* data, knockdown of *AKAP12* increased PCSK6 protein expression, paralleled by increased phosphorylation of PI3K and AKT (Fig. 6C). Subsequently, simultaneous silencing of PCSK6 in AKAP12-silenced cell lines had no effect on the expression of phosphorylated PI3K/AKT (Fig. 6D). These results confirm that expression of PCSK6 has no effect on the PI3K/AKT pathway (Fig. 6D). Meanwhile, PCSK6 silencing reduced the expression levels of inflammatory factors (Fig. 6E). Previous studies demonstrated that knockout or silencing of *AKAP12* activates the PI3K/AKT pathway [32,33]. Therefore, cell lines were constructed with *AKAP12* overexpression plasmids, which revealed that *AKAP12* overexpression inhibited the PI3K/AKT pathway (Fig. 6F). To determine whether AKAP12 regulates PCSK6 expression through the PI3K/AKT pathway, changes in PCSK6 expression in response to an AKT inhibitor were investigated. Pilot experiments have shown that the inhibitor works best at 5 min after Epidermal Growth Factor Receptor stimulation. The results demonstrated that the AKT inhibitor simultaneously inhibited the expression of p-AKT and PCSK6 (Fig. 6G), which strongly imply that activation of the PI3K/AKT pathway promotes the expression of PCSK6 (Fig. 6G). To explore the function of PCSK6 *in vivo*, small interfering RNA targeting PCSK6 were synthesized to verify the knockdown effects at the mRNA and protein levels (Fig. 6H and I). Consistently, the mRNA levels of pro-inflammatory genes in the liver were significantly reduced (Fig. 6G). The PI3K inhibitor LY294002 is reported to block the induction of PCSK6/PACE4 mRNA [15]. These results further confirmed that AKAP12 influences PCSK6 expression via the PI3K/AKT pathway.

Given the ability of PCSK6 to induce and trigger an inflammatory response, the effect of PCSK6 on ALI was investigated. $AKAP12^{\Delta hep}$ mice

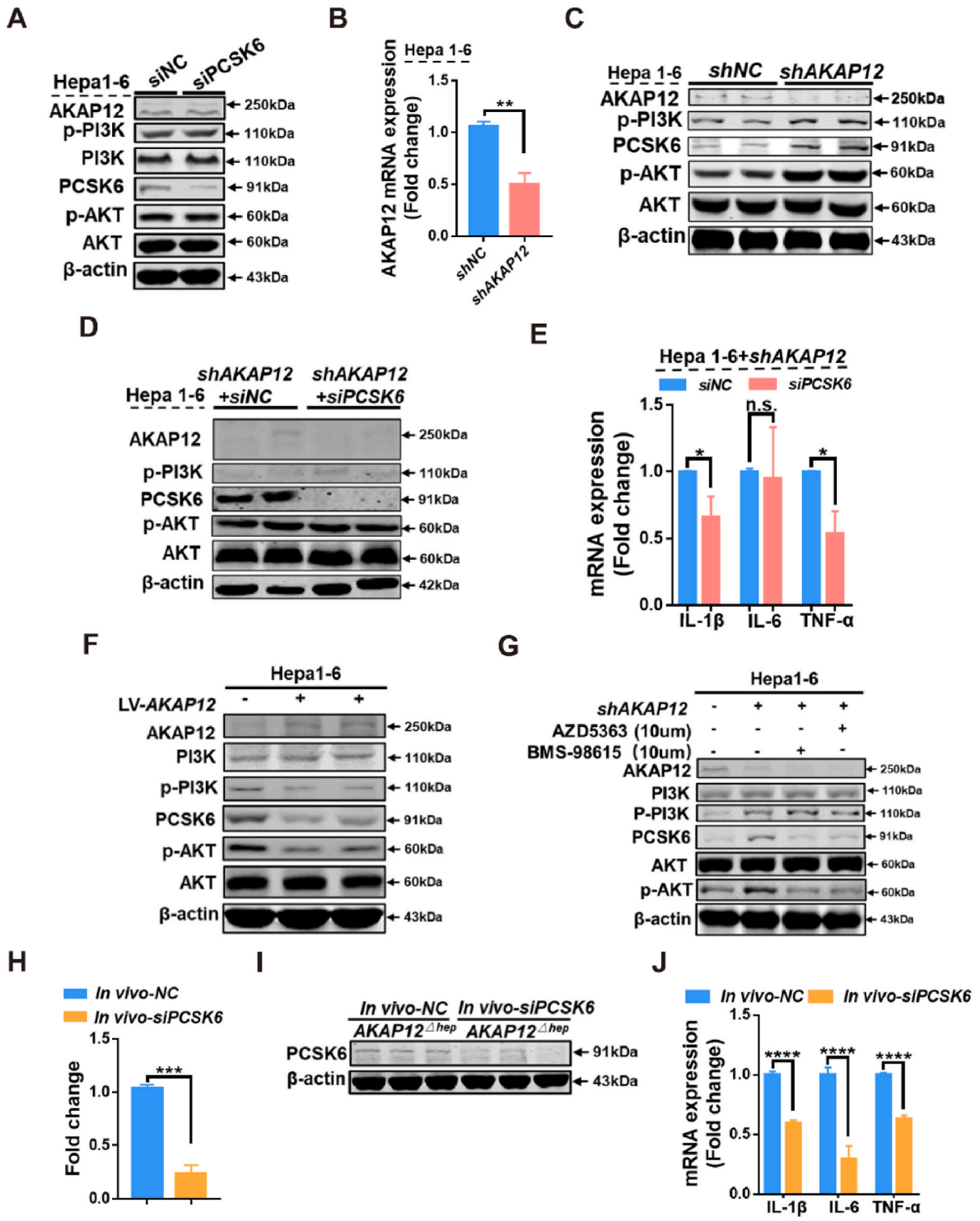

Fig. 6. AKAP12 influences PCSK6 expression via the PI3K/AKT pathway. (A) Validation of the effect of PCS6 on the PI3K/AKT pathway and AKAP12. (B) *AKAP12* mRNA expression. (C) Expression of PCSK6, PI3K, and AKT after *AKAP12* silencing. (D) Simultaneous silencing of *PCSK6* in *AKAP12*-silenced cell lines to detect PI3K/AKT expression. (E) Expression of inflammatory factors (n = 3/group). (F) Overexpression of AKAP12 verifies the expression of PI3K/AKT and PCSK6. (G) Detection of protein level expression following the use of AKT phosphorylation inhibitors. (H and I) *In vivo-siPCSK6* treatment and detection of *PCSK6* mRNA and protein expression in liver tissue. (J) Detection of inflammatory factors (*$p < 0.05$, **$p < 0.01$, ***$p < 0.001$, ****$p < 0.0001$, *n.s.* $p > 0.05$).

were intraperitoneally injected with GalN/LPS (5 μg/kg) to induce ALI and treated with *siPCSK6*. Silencing of *PCSK6* improved liver congestion and swelling in *AKAP12*$^{\Delta hep}$ mice (Supplementary Fig. 5A). The liver-to-body weight ratio and serum ALT and AST levels after *in vivo siPCSK6* treatment were significantly decreased (Supplementary Figs. 5B and C). *PCSK6* mRNA levels were significantly elevated in the livers of *AKAP12*$^{\Delta hep}$ mice with ALI (Fig. 7A). *siPCSK6* was used to inhibit *PCSK6* expression, which was validated by measuring mRNA levels (Fig. 7B). H&E staining showed that liver congestion and necrosis were significantly relieved in the *siPCSK6* group (Fig. 7C). The expression of inflammatory factors and macrophage infiltration in the liver were significantly reduced following *PCSK6* knockdown, as demonstrated by

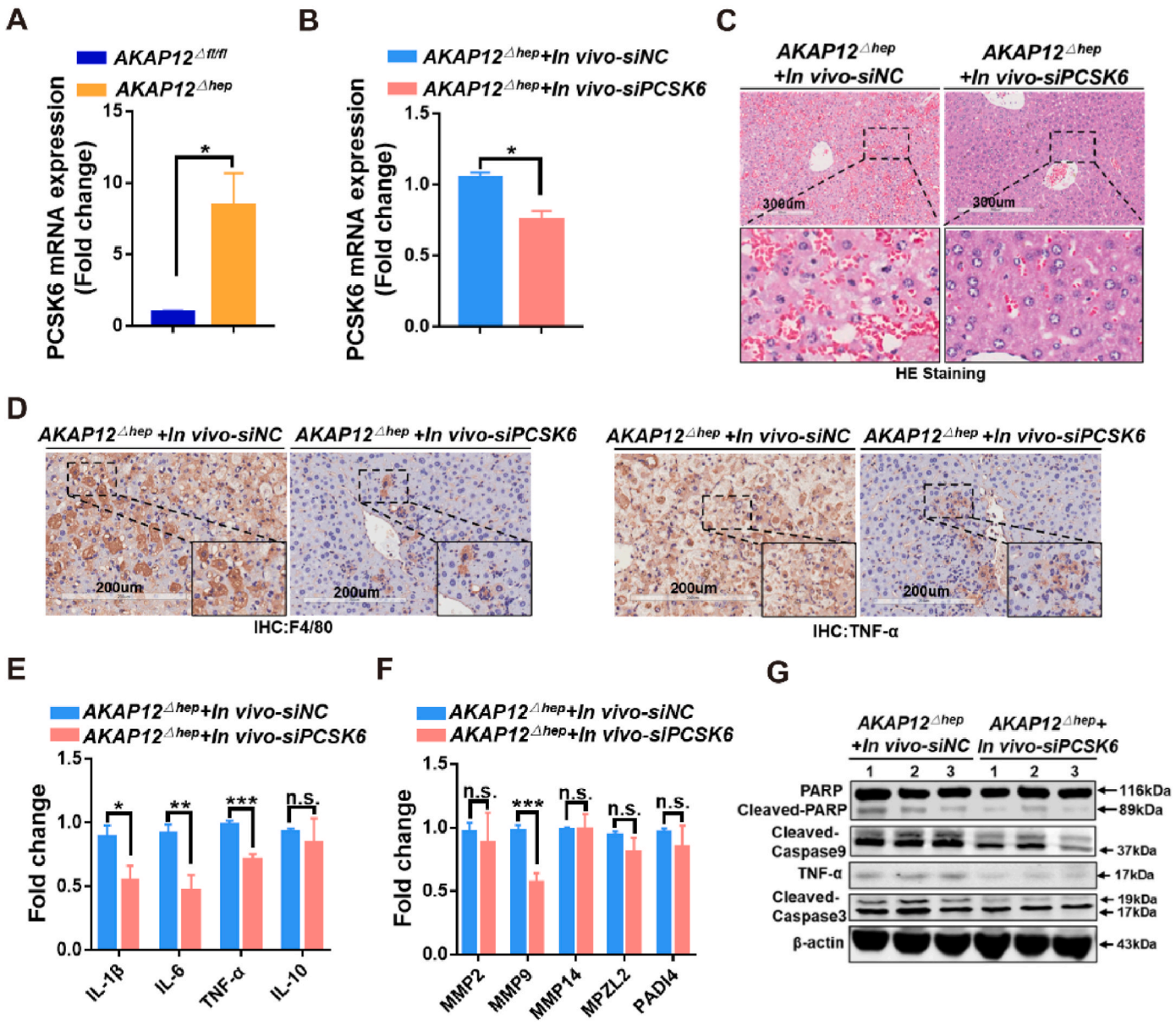

Fig. 7. ***In vivo PCSK6* effectively relieved ALI.** (A) *PCSK6* mRNA expression after AKAP12 knockout (n = 3/group). (B) Verification of the efficiency of *siPCSK6* (n = 3/group). (C) H&E staining. (D) IHC staining. (E) Expression of inflammatory factors in liver tissues (n = 3/group). (F) Detection of genes related to *PCSK6* (n = 3/group). (G) WB analysis (n = 3/group) (*$p < 0.05$, **$p < 0.01$, ***$p < 0.001$, *n.s.* $p > 0.05$).

IHC staining (Fig. 7D). In mice treated with *siPCSK6*, there was a significant decrease in the expression of MMP9, a downstream target of PCSK6, and as well as several pro-inflammatory genes (Fig. 7E and F). Further validation at the protein level found significant reductions in the expression levels of apoptotic proteins (cleaved PARP, cleaved caspase-3, cleaved capase-9) in addition to TNFα (Fig. 7G). Collectively, these results confirmed that high PCSK6 expression promoted inflammatory factor expression and macrophage infiltration, leading to more severe liver injury in the ALI model.

4. Discussion

The present study confirm that activation of the PI3K/AKT pathway in the livers of *AKAP12*$^{\Delta hep}$ mice triggers increased expression of PCSK6, which promotes macrophage infiltration and inflammatory factor expression, thereby exacerbating liver injury.

Recent studies of endothelial cells, although these cells only account for 5%–18% of liver cells, whereas hepatocytes account for about 80% [7,15,34]. The role of AKAP12 in hepatocytes remains unclear, thus further studies are warranted. The results of the present study showed that *AKAP12* deficiency promotes acute and chronic liver injury, although the specific mechanism underlying the development of liver fibrosis has yet to be elucidated. Several pathways closely related to liver fibrosis were identified and the phosphorylation levels of STAT3 and AKT were significantly increased in the liver tissues of *AKAP12*$^{\Delta hep}$ mice. Numerous studies have reported that STAT3 acts as an extracellular signaling molecule essential to chronic inflammation and promotes tumorigenesis and tumor-associated inflammation [35–37]. The PI3K/AKT signaling pathway plays an important regulatory role in the progression of liver fibrosis [37]. In addition, activation of the ERK and JNK pathways is significantly positively correlated with activation of hepatic stellate cells, which exacerbates liver fibrosis [37–40]. *AKAP12* knockout in hepatocytes activated PI3K-AKT pathway while had little or no effect on the JNK and ERK pathways. In addition, *AKAP12* knockout promoted the expression of *MMP2/9* and inflammatory factors via activation of the PI3K/AKT/PCSK6 signaling pathway, which

aggravates the progression of liver fibrosis [41,42]. Therefore, enhanced expression of PCSK6 might promote infiltration of inflammatory factors, thereby further aggravating liver fibrosis.

The results of this study showed that AKAP12 has an inhibitory effect on the expression of PCSK6. In *AKAP12*$^{\Delta hep}$ mice, the lack of *AKAP12* during the development of ALI led to activation of the PI3K/AKT pathway and increased expression of PCSK6. Knockout of *AKAP12* compromised the structural stability of hepatocytes and increased sensitivity to ROS [3,43]. Knockout of *AKAP12* accelerated PCSK6-induced inflammation, oxidative stress, and apoptosis, leading to liver damage. Abnormal expression of PCSK6 is reported to promote activation of the vascular endothelium and subsequent vascular regeneration [44,45]. Previous studies have demonstrated that PCSK6 is abnormally expressed in several solid tumors (gastric cancer, breast cancer, melanoma, etc.) [17,46,47]. PCSK6 has also been shown to enhance proliferation, migration, invasion, and inflammation of rheumatoid arthritis fibroblast-like synovial (RASF) cells via activation of the NF-κB, STAT3, and ERK1/2 signaling pathways [17,47–50]. In rheumatoid arthritis, PCSK6 is reportedly significantly increased in RASF cells [51,52]. PCSK6 stimulates secretion of the inflammatory cytokines IL-1α, IL-1β, and IL-6 in RASF cells, and increases the expression of genes related to angiogenesis, hypoxia, proliferation, and inflammation [51–54].

In addition, PCSK6 is a secreted protein, which is transported from intracellular to extracellular [17,18]. The deletion of *AKAP12* may directly affect the secretion of PCSK6, but no research has been reported and more experiments are still needed. Also, multiple pathways may be involved in the aggravation of ALI caused by *AKAP12* deletion. This paper only explores the PI3K/AKT signaling pathway, which is limited. Increased expression of PCSK6 stimulates macrophages to increase production of inflammatory factors [28,29]. In PCSK6-aggravated liver damage, activated macrophages promote the secretion of various inflammatory cytokines, thereby enhancing the inflammatory response [52]. In the present study, NAC only partially alleviated liver damage, whereas inhibition of PCSK6 expression effectively alleviated ALI. Moreover, hepatocyte-specific knockout of *AKAP12* increased apoptosis both *in vivo* and *in vitro*, which was reversed by PCSK6 knockdown. Taken together, these results demonstrate that aggravation of ALI is due to activation of PI3K/AKT and that *AKAP12* knockout enhanced PCSK6 expression, highlighting AKAP12 and PCSK6 as potential drug targets for treatment of ALI.

Ethics statements

Our animal experiments are supported and supervised by the Animal Ethics Committee of Shanghai Tenth People's Hospital (ID Number: SHDSYY-2021-3031).

Declaration of competing interest

The authors have declared that no competing interest exists.

Acknowledgments

This study was supported by grant from Special Clinical Research Project of Shanghai Municipal Health Commission (202140147) and Outstanding academic leaders plan of Shanghai (Grant No. 2018BR07). We thank the support of Shanghai Key Laboratory of Hepato-biliary Tumor Biology and Military Key Laboratory on Signal Transduction, and the Key Laboratory of Signaling Regulation and Targeting Therapy of Liver Cancer (SMMU), Ministry of Education.

Appendix A. Supplementary data

Supplementary data to this article can be found online at https://doi.org/10.1016/j.redox.2022.102328.

References

[1] H. Qasim, B. McConnell, AKAP12 signaling complex: impacts of compartmentalizing cAMP-dependent signaling pathways in the heart and various signaling systems, J. Am. Heart Assoc. 9 (13) (2020), e016615.
[2] Z. Cao, B. Singh, C. Li, N. Markham, L. Carrington, J. Franklin, Graves-Deal, R. Kennedy, E.Goldenring, J. Coffey, R. Protein kinase A-mediated phosphorylation of naked cuticle homolog 2 stimulates cell-surface delivery of transforming growth factor-α for epidermal growth factor receptor transactivation, Traffic 20 (5) (2019) 357–368.
[3] Z. Li, J. Hu, J. Guo, L. Fan, S. Wang, N. Dou, J. Zuo, S. Yu, SSeCKS/Gravin/AKAP12 inhibits pkcζ-mediated reduction of ERK5 transactivation to prevent endotoxin-induced vascular dysfunction, Cardiovasc. Toxicol. 19 (4) (2019) 372–381.
[4] M. Muramatsu, L. Gao, J. Peresie, B. Balderman, S. Akakura, I. Gelman, SSeCKS/AKAP12 scaffolding functions suppress B16F10-induced peritoneal metastasis by attenuating CXCL9/10 secretion by resident fibroblasts, Oncotarget 8 (41) (2017) 70281–70298.
[5] M. Muramatsu, S. Akakura, L. Gao, J. Peresie, B. Balderman, I. Gelman, SSeCKS/Akap12 suppresses metastatic melanoma lung colonization by attenuating Src-mediated pre-metastatic niche crosstalk, Oncotarget 9 (71) (2018) 33515–33527.
[6] R. Soh, J. Lim, R. Samy, P. Chua, B. Bay, pathology, m., A-kinase anchor protein 12 (AKAP12) inhibits cell migration in breast cancer, Exp. Mol. Pathol. 105 (3) (2018) 364–370.
[7] H. Lee, J. Choi, T. Son, E. Lee, J. Kim, S. Ryu, D. Lee, M. Jang, E. Yu, Y. Chung, I. Gelman, K. Kim, A-kinase anchoring protein 12 is downregulated in human hepatocellular carcinoma and its deficiency in mice aggravates thioacetamide-induced liver injury, Oncol. Lett. 16 (5) (2018) 5907–5915.
[8] J. Yang, H. Lee, J. Seo, J. Park, I. Gelman, E. Lo, K. Kim, Structural environment built by AKAP12+ colon mesenchymal cells drives M2 macrophages during inflammation recovery, Sci. Rep. 7 (2017) 42723.
[9] D. Yoon, C. Jeong, H. Jun, K. Chun, J. Cha, J. Seo, H. Lee, Y. Choi, B. Ahn, S. Lee, K. Kim, AKAP12 induces apoptotic cell death in human fibrosarcoma cells by regulating CDKI-cyclin D1 and caspase-3 activity, Cancer Lett. 254 (1) (2007) 111–118.
[10] P. Benz, Y. Ding, H. Stingl, A. Loot, J. Zink, I. Wittig, R. Popp, I. Fleming, AKAP12 deficiency impairs VEGF-induced endothelial cell migration and sprouting, Acta Physiol. 228 (1) (2020), e13325.
[11] B. Goeppert, P. Schmezer, C. Dutruel, Oakes, C. Renner, M. Breinig, M. Warth, A. Vogel, M. Mittelbronn, M. Mehrabi, A. Gdynia, G. Penzel, R. Longerich, T. Breuhahn, K. Popanda, O. Plass, C. Schirmacher, P. Kern, M, Down-regulation of tumor suppressor A kinase anchor protein 12 in human hepatocarcinogenesis by epigenetic mechanisms, Hepatology 52 (6) (2010) 2023–2033.
[12] S. Han, L. Wang, L. Sun, Y. Wang, B. Yao, T. Chen, R. Liu, Liu, Q.MicroRNA-1251-5p promotes tumor growth and metastasis of hepatocellular carcinoma by targeting AKAP12, Biomed. Pharmacother. 122 (2020) 109754.
[13] M. Jewell, J. Gibson, C. Guy, J. Hyun, K. Du, S. Oh, R. Premont, D. Hsu, T. Ribar, S. Gregory, A. Diehl, Single-cell RNA sequencing identifies yes-associated protein 1-dependent hepatic mesothelial progenitors in fibrolamellar carcinoma, Am. J. Pathol. 190 (1) (2020) 93–107.
[14] W. Xia, J. Ni, J. Zhuang, L. Qian, Wang, P. Wang, J. biology, c., MiR-103 regulates hepatocellular carcinoma growth by targeting AKAP12, Int. J. Biochem. Cell Biol. 71 (2016) 1–11.
[15] H. Lee, J. Choi, T. Son, H. Wee, S. Bae, J. Seo, J. Park, S. Ryu, D. Lee, M. Jang, E. Yu, Y. Chung, K. Kim, Altered AKAP12 expression in portal fibroblasts and liver sinusoids mediates transition from hepatic fibrogenesis to fibrosis resolution, Exp. Mol. Med. 50 (4) (2018) 1–13.
[16] L. Yang, J. Cao, J. Wei, Deng, J. Hou, X. Hao, E. Du, Z. Zou, L. Li, P, Antiproliferative activity of berberine in HepG2 cells inducing apoptosis and arresting cell cycle, Food Funct. 12 (23) (2021) 12115–12126.
[17] C. Weishaupt, A. Mastrofrancesco, Metze, D. Kemper, B. Stegemann, A. Picardo, M. Klein-Szanto, A. Böhm, M, Paired basic amino acid-cleaving enzyme 4 (PCSK6): an emerging new target molecule in human melanoma. Acta derm, Venereol (10) (2020) 100, adv00157.
[18] A. Bakrania, Aubé, M. Desjardins, R. Sabbagh, R. Day, R, Upregulation of PACE4 in prostate cancer is not dependent on E2F transcription factors, Can. J. Physiol. Pharmacol. 98 (7) (2020) 477–481.
[19] A. Kwiatkowska, F. Couture, S. Ait-Mohand, R. Desjardins, Dory, Y. Guérin, B. Day, R, Enhanced anti-tumor activity of the Multi-Leu peptide PACE4 inhibitor transformed into an albumin-bound tumor-targeting prodrug, Sci. Rep. 9 (1) (2019) 2118.
[20] Q. Davis, P. Xu, R.J. E, COVID-19 risk, disparities and outcomes in patients with chronic liver disease in the United States, EClinicalMedicine 31 (2021) 100688.
[21] V. Kesar, L. Channen, U. Masood, P. Grewal, J. Ahmad, N. Roth, J. Odin, Society, t. I. L. T., liver transplantation for acute liver injury in asians is more likely due to herbal and dietary supplements, Liver Transplant. 28 (2021) 188–199, https://doi.org/10.1002/lt.26260.
[22] X. Wu, S. Liu, H. Zhu, Z. Ma, X. Dai, W. Liu, Scavenging ROS to alleviate acute liver injury by ZnO-NiO@COOH, Adv. Sci. (2022), e2103982.
[23] Y. Li, C. Guo, Q. Chen, Y. Su, H. Guo, R. Liu, C. Sun, S. Mi, J. Wang, D.J. Chen, Improvement of pneumonia by curcumin-loaded bionanosystems based on platycodon grandiflorum polysaccharides via calming cytokine storm, Int. J. Biol. Macromol. 202 (2022) 691–706.
[24] Y. Li, J. Xu, D. Li, H. Ma, Y. Mu, X. Huang, L. Li, Guavinoside B from alleviates acetaminophen-induced liver injury regulating the Nrf 2 and JNK signaling pathways, Food Funct. 11 (9) (2020) 8297–8308.

[25] S. Khaled, M. Makled, M. Nader, Tiron protects against nicotine-induced lung and liver injury through antioxidant and anti-inflammatory actions in rats in vivo, Life Sci. 260 (2020) 118426.
[26] X. Pang, J. Pan, P. Gao, Y. Wang, L. Wang, B. Du, Q. Wei, A visible light induced photoelectrochemical aptsensor constructed by aligned ZnO@CdTe core shell nanocable arrays/carboxylated g-C3N4 for the detection of Proprotein convertase subtilisin/kexin type 6 gene, Biosens. Bioelectron. 74 (2015) 49–58.
[27] X. Pang, J. Pan, L. Wang, W. Ren, P. Gao, Q. Wei, Du, J.B. B, CdSe quantum dot-functionalized TiO2 nanohybrids as a visible light induced photoelectrochemical platform for the detection of proprotein convertase subtilisin/kexin type 6, Biosens. Bioelectron. 71 (2015) 88–97.
[28] V. Dianati, P. Navals, F. Couture, R. Desjardins, A. Dame, A. Kwiatkowska, Improving the selectivity of PACE4 inhibitors through modifications of the P1 residue, J. Med. Chem. 61 (24) (2018) 11250–11260.
[29] Fradet, L. Temmar, R. Couture, F. Belzile, M. Fortier, P, Evaluation of PACE4 isoforms as biomarkers in thyroid cancer, J OTOLARYNGOL-HEAD N 47 (1) (2018) 63.
[30] U. Rykaczewska, B. Suur, Röhl, S. Razuvaev, A. Lengquist, M. Sabater-Lleal, M. van der Laan, S. Miller, C. Wirka, R. Kronqvist, M. Gonzalez Diez, M. Vesterlund, M. Gillgren, P. Odeberg, J. Lindeman, J. Veglia, F. Humphries, S. de Faire, U. Baldassarre, D. Tremoli, E. Lehtiö, J. Hansson, G. Paulsson-Berne, G. Pasterkamp, G. Quertermous, T. Hamsten, A. Eriksson, P. Hedin, U, PCSK6 is a key protease in the control of smooth muscle cell function in vascular remodeling, Circ. Res. 126 (5) (2020) 571–585.
[31] H. Jiang, L. Wang, Pan, Inhibition of pro-protein convertase subtilisin/kexin type 6 has a protective role against synovitis in a rat model of rheumatoid arthritis, Mol. Med. Rep. 12 (5) (2015) 7681–7686.
[32] F. Li, T. Lu, D. Liu, C. Zhang, Y. Zhang, F. Dong, Upregulated PPARG2 facilitates interaction with demethylated AKAP12 gene promoter and suppresses proliferation in prostate cancer, Cell Death Dis. 12 (6) (2021) 528.
[33] S. Akakura, C. Huang, P. Nelson, B. Foster, I. Gelman, Loss of the SSeCKS/Gravin/AKAP12 gene results in prostatic hyperplasia, Cancer Res. 68 (13) (2008) 5096–5103.
[34] Y. Li, Q. Yu, Y. Chu, W. Wu, J. Song, X. Zhu, Q. Wang, Blockage of AKAP12 accelerates angiotensin II (Ang II)-induced cardiac injury in mice by regulating the transforming growth factor β1 (TGF-β1) pathway, Biochem. Biophys. Res. Commun. 499 (2) (2018) 128–135.
[35] J. Zhao, Y.F. Qi, Y. Yu, STAT3: a key regulator in liver fibrosis. Annals of hepatology, Ann. Hepatol. 21 (2021) 100224.
[36] D.M. Xiang, W. Sun, B.F. Ning, T.F. Zhou, X.F. Li, W. Zhong, Z. Cheng, M.Y. Xia, X. Wang, X. Deng, W. Wang, H.Y. Li, X.L. Cui, S.C. Li, B. Wu, W.F. Xie, H.Y. Wang, J. Ding, The HLF/IL-6/STAT3 feedforward circuit drives hepatic stellate cell activation to promote liver fibrosis, Gut 67 (9) (2018) 1704–1715.
[37] S.B. Su, S.Y. Qin, X.L. Xian, F.F. Huang, Q.L. Huang, Zhang Di, H. J, H.X. Jiang, Interleukin-22 regulating Kupffer cell polarization through STAT3/Erk/Akt crosstalk pathways to extenuate liver fibrosis, Life Sci. 264 (2021) 118677.
[38] Y.C. Hsieh, K.C. Lee, H.J. Lei, K.H. Lan, T.I. Huo, Y.T. Lin, C.C. Chan, B. Schnabl, Y. H. Huang, M.C. Hou, H.C. Lin, (Pro)renin receptor knockdown attenuates liver fibrosis through inactivation of ERK/TGF-β1/SMAD3 pathway. CMGH cell. Mol. Gastroenterol, Hepatology 12 (3) (2021) 813–838.
[39] C. Brenner, L. Galluzzi, O. Kepp, G. Kroemer, Decoding cell death signals in liver inflammation, J. Hepatol. 59 (3) (2013) 583–594.
[40] Q.S. Liang, J.G. Xie, C. Yu, Z. Feng, J. Ma, Y. Zhang, D. Wang, J. Lu, R. Zhuang, J. Yin, Splenectomy improves liver fibrosis via tumor necrosis factor superfamily 14 (LIGHT) through the JNK/TGF-β1 signaling pathway, Exp. Mol. Med. 53 (3) (2021) 393–406.
[41] H. Jørgensen, M. Bennett, PCSK6-Mediated regulation of vascular remodeling, Circ. Res. 126 (5) (2020) 586–588.
[42] P. He, K. Li, S. Li, T. Hu, M. Guan, F. Sun, W. Liu, Upregulation of AKAP12 with HDAC3 depletion suppresses the progression and migration of colorectal cancer, Int. J. Oncol. 52 (4) (2018) 1305–1316.
[43] P. Sandoval, D. Slentz, T. Pisitkun, F. Saeed, J. Hoffert, M. Knepper, Proteome-wide measurement of protein half-lives and translation rates in vasopressin-sensitive collecting duct cells, J. Am. Soc. Nephrol. 24 (11) (2013) 1793–1805.
[44] J. Li, J. Liu, K. Lupino, X. Liu, L. Zhang, L. Pei, Growth differentiation factor 15 maturation requires proteolytic cleavage by PCSK3, -5, and -6. Mol. Cell. Biol (21) (2018) 38.
[45] T. Kuhn, J. Knobel, S. Burkert-Rettenmaier, X. Li, I. Meyer, A. Jungmann, F. Sicklinger, J. Backs, Lasitschka, F. Müller, O. Katus, H. Krijgsveld, J. Leuschner, F, Secretome analysis of cardiomyocytes identifies PCSK6 (proprotein convertase subtilisin/kexin type 6) as a novel player in cardiac remodeling after myocardial infarction, Circulation 141 (20) (2020) 1628–1644.
[46] Patel, A. García-Closas, M. Olshan, A. Perou, C. Troester, M. Love, M. Bhattacharya, A, Gene-level germline contributions to clinical risk of recurrence scores in black and white patients with breast cancer, Cancer Res. 82 (1) (2022) 25–35.
[47] J. Chen, Y. Li, J. Wu, Y. Liu, S. Kang, Whole-exome sequencing reveals potential germline and somatic mutations in 60 malignant ovarian germ cell tumors, Biol. Reprod. 105 (1) (2021) 164–178.
[48] X. Zhao, X. Zhang, Z. Wu, J. Mei, L. Li, Y. Wang, Up-regulation of microRNA-135 or silencing of PCSK6 attenuates inflammatory response in preeclampsia by restricting NLRP3 inflammasome, Mol. Med. 27 (1) (2021) 82.
[49] G. Oroszlán, Dani, R. Végh, B. Varga, D. Ács, A. Pál, G. Závodszky, P. Farkas, H. Gál, P. Dobó, J, Proprotein convertase is the highest-level activator of the alternative complement pathway in the blood, J. Immunol. 206 (9) (2021) 2198–2205.
[50] Testa, G. Staurenghi, E. Giannelli, S. Sottero, B. Gargiulo, S. Poli, G. Gamba, P. Leonarduzzi, G, Up-regulation of PCSK6 by lipid oxidation products: a possible role in atherosclerosis, Biochimie 181 (2021) 191–203.
[51] H. Jiang, L. Wang, F. Wang, J. Pan, Proprotein convertase subtilisin/kexin type 6 promotes in vitro proliferation, migration and inflammatory cytokine secretion of synovial fibroblast-like cells from rheumatoid arthritis via nuclear-κB, signal transducer and activator of transcription 3 and extracellular signal regulated 1/2 pathways, Mol. Med. Rep. 16 (6) (2017) 8477–8484.
[52] F. Wang, L. Wang, H. Jiang, X. Chang, J. Pan, Inhibition of PCSK6 may play a protective role in the development of rheumatoid arthritis, J. Rheumatol. 42 (2) (2015) 161–169.
[53] J. Wylie, J. Ho, S. Singh, D. McCulloch, S. Apte, Adamts5 (aggrecanase-2) is widely expressed in the mouse musculoskeletal system and is induced in specific regions of knee joint explants by inflammatory cytokines, J. Orthop. Res. 30 (2) (2012) 226–233.
[54] Khoury, E. Kinaneh, S. Aronson, D. Amir, O. Ghanim, D. Volinsky, N. Azzam, Z. Abassi, Z, Natriuretic peptides system in the pulmonary tissue of rats with heart failure: potential involvement in lung edema and inflammation, Oncotarget 9 (31) (2018) 21715–21730.